M.I. Boiko, A.V. Makogon

Features of distribution of electric field strength and current density in the reactor during treatment of liquid media with high-voltage pulse discharges

Purpose. *Development and use of a mathematical model of the stages of formation of high-voltage pulse discharges in gas bubbles in the discharge gap «rod-plane» to identify the features of the electric field intensity distribution in the reactor and determine the current density in the load during disinfection and purification of liquid media by high-voltage pulse discharges and find the most rational treatment.* ***Methodology***. *To achieve this goal, we used computer modeling using the finite element method as a method of numerical analysis. An experimental reactor model was created that takes into account the dynamics of discharges in gas bubbles in water. The equations describing the system include the generalized Ampere equation, the Poisson equation and the electric displacement equation, taking into account the corresponding initial and boundary conditions, as well as the properties of materials. The dependence of the potential of a high-voltage electrode on time has the form of a damped sinusoid, and the specific electrical conductivity in a gas bubble is a function of time. Processes occurring at the front of the voltage pulse from 0 to 20 ns are considered.* ***Results***. *It is shown that with an increase in conductivity and high-voltage potential to amplitude values in a gas bubble, the electric field strength in the water layer in the reactor reaches 70 kV/cm, and it is in the water layer that there is a strong electric field. The calculations show that already by 19th ns the density of conduction currents in water prevails over that of displacement currents. At the same time, additional inclusions in the water significantly affect the distribution of electric field strength and current density, creating a significant difference in their values at the boundaries of the interface between the bubble, conductive element and water.* ***Originality***. *A simulation of the dynamics of transient discharge processes in a gas bubble and a layer of water with impurities was carried out, including an analysis of the distribution of the electric field strength and current density in a system with rod-plane electrodes in the phase transition section of a gas bubble-water. This approach allows us to reveal the features of processes in reactors and to investigate the influence of phase transitions on the distribution of electrophysical quantities.* ***Practical value***. *Computer simulations confirm the prospect of using nanosecond discharges generated in gas bubbles within a volume of water for widespread industrial use and are of great interest for further experimental and theoretical research.* References 25, figures 9.
Key words: **reactor, electric field strength, conductivity current density, displacement current density, discharge in a gas bubble in water, inclusion in water.**

***Мета.** Розробка та використання математичної моделі стадій формування високовольтних імпульсних розрядів у газових бульках в розрядному проміжку «стрижень-площина» для виявлення особливостей розподілу напруженості електричного поля в реакторі і визначення густини струму в навантаженні при знезаражуючій обробці і очищенні рідких середовищ високовольтними імпульсними розрядами та знаходження найбільш раціональних режимів обробки. **Методика.** Для досягнення поставленої мети ми використовували комп'ютерне моделювання за допомогою методу скінченних елементів як методу чисельного аналізу. Створено модель експериментального реактора, що враховує динаміку розрядів у газових бульках у воді. Рівняння, що описують систему, включають узагальнене рівняння Ампера, рівняння Пуассона і рівняння електричного зміщення, з урахуванням відповідних початкових і граничних умов, а також властивостей матеріалів. Залежність потенціалу високовольтного електрода від часу має форму затухаючої синусоїди, а питома електропровідність у газовій бульці є функція часу. Розглянуто процеси, що протікають на фронті імпульсу напруги від 0 до 20 нс. **Результати.** Показано, що зі зростанням провідності та високовольтного потенціалу до амплітудних значень у газовій бульці, напруженість електричного поля в шарі води в реакторі досягає значень 70 кВ/см, і саме в шарі води існує сильне електричне поле. З розрахунків випливає, що біля 19-ої нс, густина струмів провідності у воді вже перевершує густину струмів зміщення. При цьому додаткові включення в воді істотно впливають на розподіл напруженості електричного поля та густини струму, створюючи значне збільшення в їх значеннях на границях розділу середовищ між бульбашкою, провідним елементом та водою. **Наукова новизна.** Проведено моделювання динаміки швидкоплинних процесів розряду в газовій бульці та шарі води з домішками, включно з аналізом розподілу напруженості електричного поля і густини струму в системі з електродами «стрижень-площина» в ділянці фазового переходу газова булька-вода. Цей підхід дозволяє розкрити особливості процесів в реакторах і дослідити вплив фазових переходів на розподіл електрофізичних величин. **Практична цінність.** Комп'ютерне моделювання підтверджує перспективу застосування наносекундних розрядів, що генеруються в газових бульках усередині об'єму води, для широкого промислового використання і становлять великий інтерес для подальших експериментальних і теоретичних досліджень. Бібл. 25, рис. 9.*
Ключові слова: **реактор, напруженість електричного поля, густина струмів провідності, густина струмів зміщення, розряд у газовій бульці у воді, включення у воді.**

Introduction. Modern requirements for wastewater treatment require the development of effective means of destruction of organic substances that are resistant to the action of traditional oxidizers. Another component of the problem is the general requirements of decarbonization of the economy, and the success of their solution also applies to wastewater treatment [1-3]. It is especially important here to avoid long processes of biochemical decomposition of organic substances, accompanied by the formation of CH_4, as a gas that has a significantly higher coefficient of contribution to the greenhouse effect, compared to CO_2. Among the technological alternatives to the traditional technologies of natural and reagent oxidation of compounds contained in wastewater, electrophysical technologies stand out, the tools of which are factors caused by the action of ionizing radiation [4], plasma flows [5], and high-voltage discharges [6]. Prospects for the successful practical implementation of each of the indicated directions, in that the resource for their optimization consists in establishing ways of more fully using the energy of the field effect on the object of

destruction (bacteria, viruses, organic compounds) and establishing the role of concomitant factors generated as a result of high-voltage electric discharges in water (acoustic pulses, local temperature increases, secondary radiation). Thus, during the treatment of wastewater by methods based on high-voltage electric discharges, various physical and chemical processes occur: the formation of oxidants, including hydroxyl radicals, ozone, the occurrence of shock waves, ultraviolet radiation, strong electric fields [7-12]. The hydroxyl radical OH^- itself acts as a natural oxidant, exhibits high biocidal activity, is capable of effectively destroying pollutants, inactivating bacteria, viruses, yeast, and oxidizing organic and inorganic compounds [13-15].

The strong electric field in the discharge accelerates the electrons, increasing their ability to ionize atoms and molecules, which leads to an avalanche-like increase in the number of free charge carriers, increasing the current, causing more efficient gas ionization and the formation of more active particles. Under the influence of strong pulse electric fields, the breaking of chemical bonds in molecules can occur, as well as their dissociation, which leads to an increase in the number of free atoms and radicals that can participate in chemical reactions [16]. Also, electric fields, the action of which lasts from micro to nanoseconds with strength of the order of 10-100 kV/cm in the form of pulses of electric field strength of various shapes, effectively inactivate microorganisms, while the primary color, taste, and nutritional value of juices, wines, and dairy products are preserved after their processing [17-21]. In our works [21-23], it was substantiated that the effectiveness of the high-voltage discharge action significantly increases under the condition of injection into the discharge zone of a flow of air bubbles.

The complexity of rapid discharge processes makes it difficult to fully understand the dynamics of the discharge inside the bubble and the water layer, namely, how the electric field strength and current density are distributed in the reactor in the area of the phase transition between gas bubble and water using experimental studies.

The goal of the article is to develop and use a mathematical model of the stages of formation of high-voltage pulse discharges in gas bubbles in the "rod-plane" discharge gap to identify the features of the electric field strength distribution in the reactor and determine the current density in the load during disinfection and cleaning of liquid media with high-voltage pulse discharges and finding the most rational processing modes.

Description of the mathematical model of a reactor for wastewater treatment using high-voltage discharges in gas bubbles in it. Figure 1 shows a model of an experimental reactor for water treatment using discharges in gas bubbles in Cartesian coordinate systems (the dimensions along the axes are given in mm).

The boundary 7-8-9 and 5-11 is a system of copper electrodes ($\sigma = 6{\cdot}10^7$ S/m): high-voltage rod electrode with radius of curvature of 0.5 mm, low-voltage flat electrode. The gas is supplied to the area of the high-voltage electrode 1, where discharges occur directly. Electrode 1 is fixed in the dielectric housing 4 ($\varepsilon = 2.3$, $\sigma = 1{\cdot}10^{-12}$ S/m). The interelectrode space contains a gas

bubble 2 ($\varepsilon = 1$) and a model water solution 3 ($\varepsilon = 81$, $\sigma = 0.125$ S/m).
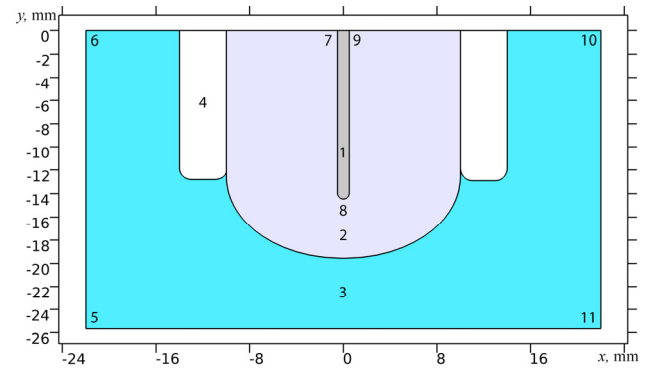

Fig. 1. Model of a reactor for wastewater treatment using high-voltage discharges in gas bubbles in water

The finite element method was used during computer modeling of the formation and development over time of a pulse electrical discharge in a gas bubble inside water.

The initial system of equations:

$$\begin{cases} \boldsymbol{J} = \sigma \cdot \boldsymbol{E} + \partial \boldsymbol{D}/\partial t; \\ \boldsymbol{E} = -\nabla V; \\ \boldsymbol{D} = \varepsilon_0 \cdot \varepsilon \cdot \boldsymbol{E}, \end{cases} \quad (1)$$

where $\boldsymbol{J}$ is the total current density, σ is the specific electrical conductivity of the material, $\boldsymbol{E}$ is the electric field strength, ε_0 is the dielectric permittivity of the vacuum, ε is the relative dielectric permittivity of the material, $\boldsymbol{D}$ is the electric displacement vector of the dielectric, and V is the electric scalar potential.

In the calculation domain, the condition of continuity of the current is fulfilled: $\nabla \boldsymbol{J} = 0$.

The superimposition of the spatial mesh in the domain of the high-voltage electrode and the gas bubble-water phase transition in the reactor is shown in Fig. 2. A triangular mesh with typical element sizes from $8.8{\cdot}10^{-4}$ mm to 0.44 mm is set in the entire domain.
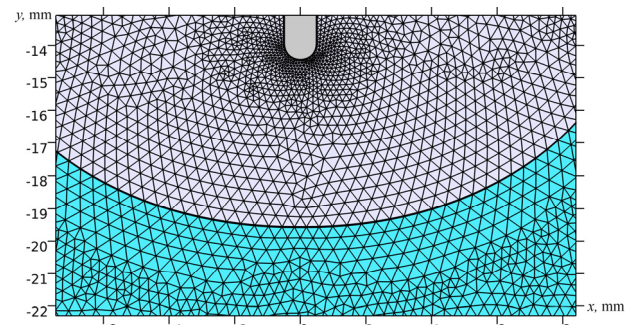

Fig. 2. Superimposition of a spatial mesh in the domain of the gas bubble-water phase transition

Dependence of the potential of the high-voltage electrode on time (boundary 7-8-9) in Fig. 3,a has the form of a decaying sinusoid, which is an approximation of the obtained experimental oscillograms of Fig. 3,b.

Figure 3,b shows experimental oscillograms of nanosecond discharges in gas bubbles in water [23]. The voltage amplitude (curve 1) reaches 30 kV, and the

current amplitude (curve 2) – 100 A, the scale along the time axis is 50 ns/div. The scale along the process axis for current oscillograms is 32 A/div, and for voltage oscillograms – 7.9 kV/div.
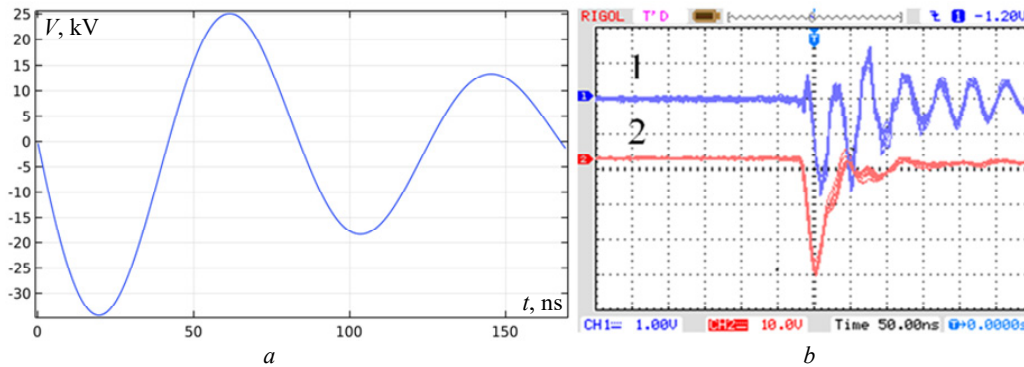

Fig. 3. Model and experimental pulses in the reactor: *a* − dependence of the potential of the high-voltage electrode on time;
b − oscillograms of nanosecond pulses: 1 − voltage pulse, 2 − current pulse

The potential of the low-voltage electrode $V = 0$ (boundary 5-11).

The calculation was performed in the time domain from 0 to 170 ns, with a time step of 0.1 ns.

At zero time, the voltage at all points in the reactor is $V_0 = 0$.

At the boundary 5-6-7, 9-10-11 of the calculation domain, the boundary condition of electrical isolation is set:

$$\boldsymbol{n} \cdot \boldsymbol{J} = 0, \qquad (2)$$

where $\boldsymbol{n}$ is the vector normal to the surface through which the current passes, $\boldsymbol{J}$ is the current density vector.

This boundary condition means that electric current does not flow across boundaries. The projection of the current density vector on the normal to the surface describes the current density flowing perpendicular to this surface. If the projection is equal to 0, then this indicates the absence of a current perpendicular to the surface. This state corresponds to the boundary conditions of isolation, where charge transfer does not occur at the interface of two media. The potential distribution must be continuous at the interface and the same on both sides of the interface.

Specific electrical conductivity was determined in the model as a function of time to illustrate the influence of ionization processes occurring in the gas bubble under the action of an electric field (Fig. 4).
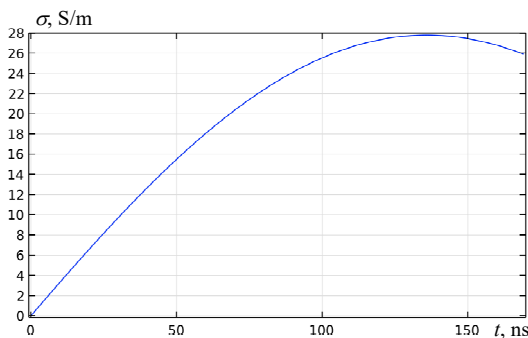

Fig. 4. Specific electrical conductivity in a gas bubble as a function of time

In Fig. 4, specific electrical conductivity changes as follows. At the zero moment of time, the specific electrical conductivity of the gas bubble is 2 orders of magnitude lower than that of water. Gas is a dielectric and contains almost no free charges, so its conductivity is low. On the other hand, wastewater has conductivity due to various ions and minerals dissolved in it, which are carriers of electrical charge and can easily conduct current. As the potential of the high-voltage electrode increases, the electric field strength increases, which activates the movement of free electrons in the bubble. These electrons ionize neutral gas atoms, generating additional free charges. Thus, the number of free charges increases dramatically, which significantly increases gas conductivity. In the model, the conductivity of gas becomes greater than that of water by about 52 times.

Simulation results and their discussion. The processes taking place at the front of the voltage pulse from 0 to 20 ns, when the potential on the high-voltage electrode increases from 0 to the amplitude value, are considered.

In the model, the vector $\boldsymbol{E}$ in two-dimensional space is represented as $\boldsymbol{E} = (E_x, E_y)$, where E_x is the component of the vector along the *x*-axis, and E_y is the component of the vector along the *y*-axis. Thus, to calculate the length of the vector $\boldsymbol{E}$, we take the square root of the sum of the squares of its components. After calculating the length of the vector, we get the modulus of the electric field strength.

Figure 5 shows the distribution of the *y*-component of the electric field strength in the reactor.

Figure 5 demonstrates that at the initial moments of time on the (front) of the pulse, the electric field strength near the rod reaches 22 kV/cm, and that with the growth of the bubble conductivity and high-voltage potential to amplitude values, the electric field strength on the water layer reaches 62 kV/cm.

In addition, impurities are introduced into the model water in the reactor, which may be present in the water being treated and contribute to the distribution of the electric field strength and current density, the intersection of which in the plane where the calculations are carried out has the shape, for example, of moist air bubbles in the form of circles with diameter of 1 mm ($\varepsilon = 1$, $\sigma = 0.01$ S/m), copper particles in the form of a square with side of 1 mm and specific electrical conductivity of $1 \cdot 10^7$ S/m.
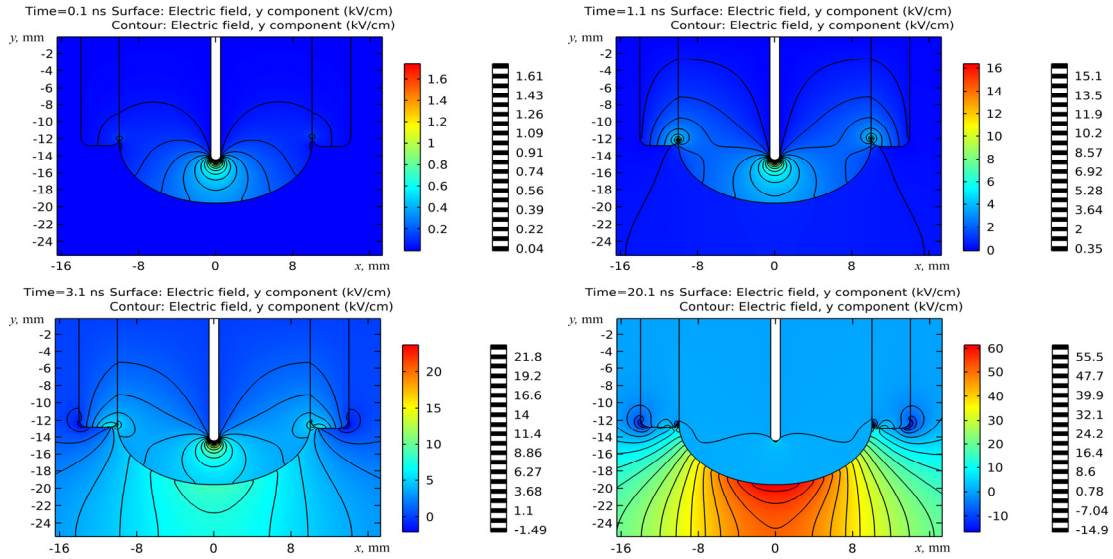
Fig. 5. Distribution of the *y*-component of the electric field strength in the reactor

Figure 6 shows the distribution of the electric field strength with additional impurities in water at the time of 20.1 ns.
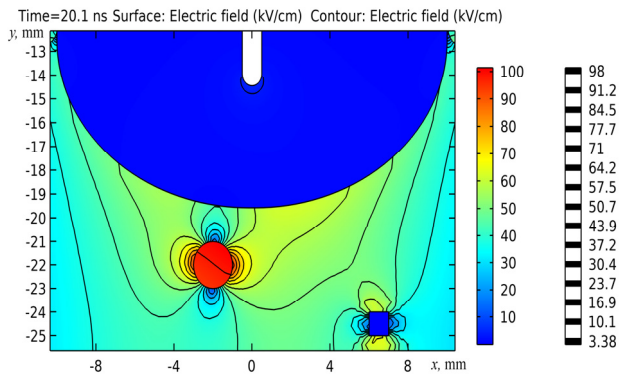

Fig. 6. Distribution of electric field strength in a reactor with impurities in water

Figure 6 demonstrates the distribution of the electric field strength in the Cartesian coordinate system. Here, at 20.1 ns, the electric field strength in the gas bubble of moist air in water reaches 102 kV/cm, in the water layer itself – up to 70 kV/cm. A gas bubble in water is a dielectric. At the interface with water, the electric field strength increases sharply, being distributed inversely proportional to the ratio of relative dielectric permittivities. At the time of 20.1 ns, it can be observed that the value of the electric field in the bubble and in the water at the interface of the media differs by a factor of 10 in some directions.

Modeling of the pre-breakdown distribution of the electric field strength at the specific conductivity of the bubble (in the domain of the high-voltage electrode) of $1 \cdot 10^{-5}$ S/m is shown in Fig. 7.

The process of forming a discharge in a gas bubble can be divided into two stages: *pre-breakdown*, when the gas bubble acts as a dielectric at the initial moments of the process, and *breakdown*, when the gas bubble goes into a conductive state. Due to the increase in the electric field strength, the ionization processes are started and the conductivity increases sharply. The breakdown moment
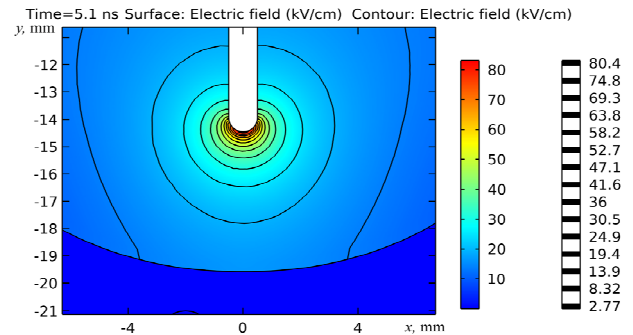

Fig. 7. Distribution of electric field strength in the domain of the high-voltage electrode according to the specific electrical conductivity of the gas bubble of $1 \cdot 10^{-5}$ S/m

strongly depends on the electric field strength amplitudes, which are affected by the radius of curvature of the rod electrode and the electrical strength of the medium in the discharge gap. During a nanosecond pulse in the gas bubble (Fig. 7), the following electric field strength values were obtained: near the rod – 82 kV/cm, in the bubble itself – up to 40 kV/cm at time of 5.1 ns. The picture of the processes during the breakthrough period itself is similar to the picture of the electric field strength distribution in Fig. 6 according to the specific electrical conductivity of the bubble of $1 \cdot 10^{4}$ S/m, where it is shown that a strong electric field exists precisely in the water layer. A copper particle also distorts the electric field in water (up to 60 kV/cm). Such a distortion can additionally lead to the development of high-intensity factors, microparticles in water.

When a strong electric field exists in water itself, various physicochemical phenomena occur there, such as ionization, dissociation of water molecules into hydroxyl radicals and hydrogen, as well as the formation of gas microbubbles with characteristic dimensions of $10^{-6} – 10^{-5}$ m as in water, as well as in the domain of its contact with the plasma and metal electrodes [24], where microdischarges such as partial discharges occur in gas inclusions in solid dielectrics. At the interface of two dielectrics with different dielectric permittivities, the electric field generates a mechanical force that is directed

perpendicular to the interface and directed toward the dielectric with a lower dielectric permittivity. This force acts regardless of the direction of the electric field strength [25]. We meant that viruses and the membranes of the cells of microorganisms in the treated water are also the dielectrics with a relative dielectric permittivity $\varepsilon = 2 - 4$. During contact of this membrane with water in strong electric field, its sharp increase occurs, which can reach 60 kV/mm. Such an increase in the electric field strength on inhomogeneities in the treated water triggers additional processes of impact ionization by electrons. Collectively, this ultimately leads to a higher degree of disinfection and purification of wastewater.

Figure 8 shows the distribution of conductivity current density.

Up to 20 ns, the conductivity current density near the rod reaches 320 A/cm^2, in the water itself 50-70 A/cm^2, the presence of additional inclusions leads to a 10 time increase in the current density values at the interface between the water medium and these inclusions.

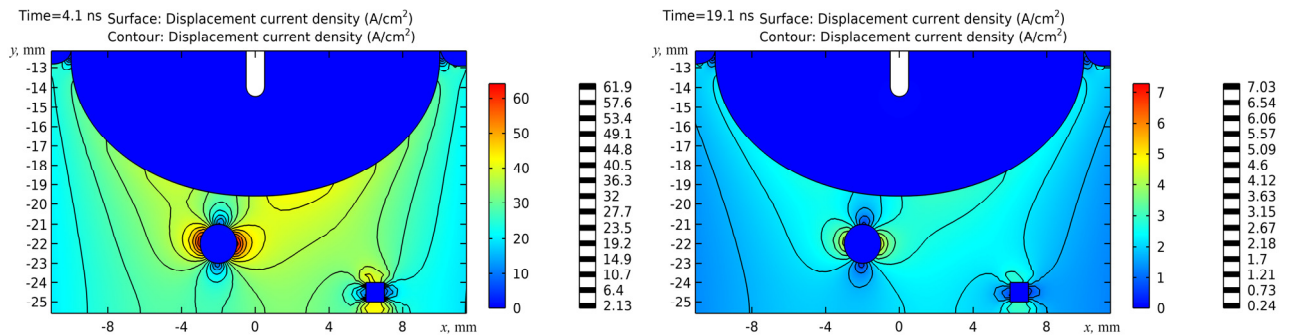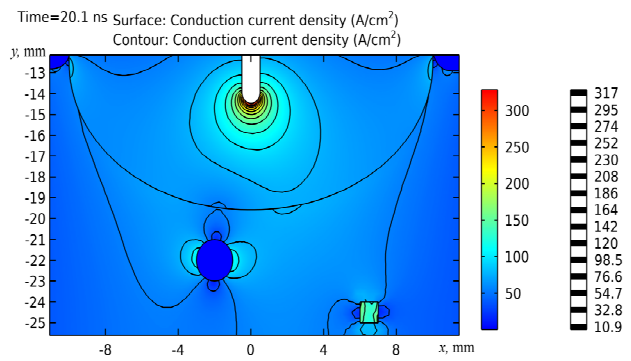Figure 9 shows the simulation of displacement currents in water.

Fig. 8. Distribution of conductivity current density in a sewage treatment reactor

The displacement current density is estimated as a value directly proportional to the rate of change of electrical induction. In Fig. 9, the maximum density of displacement currents in water reaches 62 A/cm^2 at time of 4.1 ns. Further, it follows from the calculations that up to approximately 19 ns after the start of the discharge process, the conductivity currents in water become larger compared to the displacement currents.

Fig. 9. Modeling of displacement currents in water in a reactor for wastewater treatment

Conclusions.

1. Calculations show that with the growth of conductivity and high potential in the gas bubble to amplitude values, a strong electric field (with strength of up to 70 kV/cm) is created in the water layer. At the same time, additional inclusions contribute to the distortion of the electric field. The values of the electric field strengths in the bubble, conductive inclusion, and water can differ by a factor of 10.

2. At the beginning of the discharge process in the reactor, when there is no gas discharge plasma in the gas bubble near the high-voltage electrode, and the bubble is a dielectric, the moment of breakdown start depends strongly on the amplitude of the electric field strength, which is affected by the radius of curvature of the rod electrode, and the electrical strength of the discharge gap. The higher the rate of voltage rise and the smaller the radius of curvature, the higher the breakdown strength in the nanosecond time range can be obtained (up to 82 kV/cm).

3. In the nanosecond time range, the conductivity current density near the rod exceeds the density in the water itself by 5 or more times, reaching values of 300 A/cm^2 or more. At the same time, additional inclusions also introduce a distortion of the current densities at the interface of the media with a 10-time increase. It follows from the calculations that already approximately by 19th ns after the start of the discharge process, the density of conductivity currents in water exceeds the density of displacement currents.

4. High-voltage nanosecond discharges, which are created in gas bubbles inside the volume of water or in a gas environment near the water surface, have good prospects for wide industrial use in disinfection, wastewater treatment, decarbonization of the economy and are of great interest for further experimental and theoretical research.

Conflict of interest. The authors declare no conflict of interest.

REFERENCES
1. Doorn M.R.J., Towprayoon S., Vieira S.M.M., Irving W., Palmer C., Pipatti R., Wang C. Wastewater treatment and discharge. *2006 IPCC Guidelines for National Greenhouse Gas Inventories*, 2006, 28 p.
2. He Y., Li Y., Li X., Liu Y., Wang Y., Guo H., Hou J., Zhu T., Liu Y. Net-zero greenhouse gas emission from wastewater treatment: Mechanisms, opportunities and perspectives. *Renewable and Sustainable Energy Reviews*, 2023, vol. 184, art. no. 113547. doi: https://doi.org/10.1016/j.rser.2023.113547.
3. Ranieri E., D'Onghia G., Lopopolo L., Gikas P., Ranieri F., Gika E., Spagnolo V., Ranieri A.C. Evaluation of greenhouse gas emissions from aerobic and anaerobic wastewater treatment plants in Southeast of Italy. *Journal of Environmental Management*, 2023, vol. 337, art. no. 117767. doi: https://doi.org/10.1016/j.jenvman.2023.117767.

4. Bojanowska-Czajka A. Application of Radiation Technology in Removing Endocrine Micropollutants from Waters and Wastewaters – A Review. *Applied Sciences*, 2021, vol. 11, no. 24, art. no. 12032. doi: https://doi.org/10.3390/app112412032.

5. Yusuf A., Amusa H.K., Eniola J.O., Giwa A., Pikuda O., Dindi A., Bilad M.R. Hazardous and emerging contaminants removal from water by plasma-based treatment: A review of recent advances. *Chemical Engineering Journal Advances*, 2023, vol. 14, art. no. 100443. doi: https://doi.org/10.1016/j.ceja.2023.100443.

6. Sato M. Environmental and biotechnological applications of high-voltage pulsed discharges in water. *Plasma Sources Science and Technology*, 2008, vol. 17, no. 2, art. no. 024021. doi: https://doi.org/10.1088/0963-0252/17/2/024021.

7. McQuaid H.N., Rutherford D., Mariotti D., Maguire P.D. Generation and delivery of free hydroxyl radicals using a remote plasma. *Plasma Sources Science and Technology*, 2023, vol. 32, no. 1, art. no. 015005. doi: https://doi.org/10.1088/1361-6595/acb07f.

8. Gou X., Yuan D., Wang L., Xie L., Wei L., Zhang G. Enhancing ozone production in dielectric barrier discharge utilizing water as electrode. *Vacuum*, 2023, vol. 212, art. no. 112047. doi: https://doi.org/10.1016/j.vacuum.2023.112047.

9. Joubert V., Cheype C., Bonnet J., Packan D., Garnier J.-P., Teissié J., Blanckaert V. Inactivation of Bacillus subtilis var. niger of both spore and vegetative forms by means of corona discharges applied in water. *Water Research*, 2013, vol. 47, no. 3, pp. 1381-1389. doi: https://doi.org/10.1016/j.watres.2012.12.011.

10. Lukes P., Clupek M., Babicky V., Sunka P. Ultraviolet radiation from the pulsed corona discharge in water. *Plasma Sources Science and Technology*, 2008, vol. 17, no. 2, art. no. 024012. doi: https://doi.org/10.1088/0963-0252/17/2/024012.

11. Zeng M.J., Qu Z.G., Zhang J.F. Negative corona discharge and flow characteristics of a two-stage needle-to-ring configuration ionic wind pump for temperature and relative humidity. *International Journal of Heat and Mass Transfer*, 2023, vol. 201, art. no. 123561. doi: https://doi.org/10.1016/j.ijheatmasstransfer.2022.123561.

12. Boshko I., Kondratenko I., Zabulonov Y.L., Charnyi D.V., Onanko Y., Marynin A., Krasnoholovets V. The study of treatment of water with a high concentration of cod by pulse dielectric barrier discharge on the surface of the liquid. *Geochemistry of Technogenesis*, 2020, vol. 32, no. 4, pp. 65-70. doi: https://doi.org/10.15407/geotech2020.32.065.

13. Khan Z.U.H., Gul N.S., Sabahat S., Sun J., Tahir K., Shah N.S., Muhammad N., Rahim A., Imran M., Iqbal J., Khan T.M., Khasim S., Farooq U., Wu J. Removal of organic pollutants through hydroxyl radical-based advanced oxidation processes. *Ecotoxicology and Environmental Safety*, 2023, vol. 267, art. no. 115564. doi: https://doi.org/10.1016/j.ecoenv.2023.115564.

14. Gershman S., Mozgina O., Belkind A., Becker K., Kunhardt E. Pulsed Electrical Discharge in Bubbled Water. *Contributions to Plasma Physics*, 2007, vol. 47, no. 1–2, pp. 19-25. doi: https://doi.org/10.1002/ctpp.200710004.

15. Yasuoka K., Sato K. Development of Repetitive Pulsed Plasmas in Gas Bubbles for Water Treatment. *International Journal of Plasma Environmental Science and Technology*, 2009, vol. 3, no. 1, pp. 22-27. doi: https://doi.org/10.34343/ijpest.2009.03.01.022.

16. Raizer Yu.P. *Gas Discharge Physics*. Berlin, Springer, 1991. 449 p.

17. Zare F., Ghasemi N., Bansal N., Hosano H. Advances in pulsed electric stimuli as a physical method for treating liquid foods. *Physics of Life Reviews*, 2023, vol. 44, pp. 207-266. doi: https://doi.org/10.1016/j.plrev.2023.01.007.

18. Mohamed M.E.A., Eissa A.H.A. Pulsed Electric Fields for Food Processing Technology. *Structure and Function of Food Engineering*, 2012, pp. 275-306. doi: https://doi.org/10.5772/48678.

19. Bahrami A., Moaddabdoost Baboli Z., Schimmel K., Jafari S.M., Williams L. Efficiency of novel processing technologies for the control of Listeria monocytogenes in food products. *Trends in Food Science & Technology*, 2020, vol. 96, pp. 61-78. doi: https://doi.org/10.1016/j.tifs.2019.12.009.

20. Martinez J.M., Delso C., Alvarez I., Raso J. Pulsed electric field-assisted extraction of valuable compounds from microorganisms. *Comprehensive Reviews in Food Science and Food Safety*, 2020, vol. 19, no. 2, pp. 530-552. doi: https://doi.org/10.1111/1541-4337.12512.

21. Boyko N.I., Makogon A.V. Generator of high-voltage nanosecond pulses with repetition rate more than 2000 pulses per second for water purification by the discharges in gas bubbles. *Technical Electrodynamics*, 2018, no. 4, pp. 37-40. doi: https://doi.org/10.15407/techned2018.04.037.

22. Boyko N.I., Makogon A.V. High voltage plant with 3 MW pulse power for disinfection flow of water by nanosecond discharges in gas bubbles. *Technical Electrodynamics*, 2020, no. 5, pp. 80-83. doi: https://doi.org/10.15407/techned2020.05.080.

23. Boyko N.I., Makogon A.V. The micro- and nanosecond discharges in gas bubbles for water disinfection and purification. *Electrical Engineering & Electromechanics*, 2019, no. 3, pp. 50-54. doi: https://doi.org/10.20998/2074-272X.2019.3.08.

24. Korobeinikov S.M. *Preliminary processes in rare dielectrics under the influence of pulsed voltage have been proven*. Candidate of Technical Sciences Thesis. Novosibirsk, 1983. 24 p. (Rus).

25. Poplavko Yu.M. *Physics of Dielectrics*. Kyiv, NTUU «KPI» Publ., 2015. 572 p. (Ukr).

M.I. Boiko[1]*, Doctor of Technical Sciences, Professor,*
A.V. Makogon[2]*, PhD, Senior Researcher,*
[1] National Technical University «Kharkiv Polytechnic Institute»,
2, Kyrpychova Str., Kharkiv, 61002, Ukraine,
e-mail: qnaboyg@gmail.com
[2] Institute of Electrophysics & Radiation Technologies
National Academy of Sciences of Ukraine,
28, Chernyshevsky Str., Kharkiv, 61002, Ukraine,
e-mail: artemmak1991@gmail.com (Corresponding Author)